CHAPTER

8

Synchrotron small-angle X-ray scattering and electron microscopy characterization of structures and forces in microtubule/Tau mixtures

Peter J. Chung*,[1,2], Chaeyeon Song*,[3], Herbert P. Miller[†], Youli Li[‡], Uri Raviv[§], Myung Chul Choi[¶], Leslie Wilson[†], Stuart C. Feinstein[†], Cyrus R. Safinya*,[1]

*University of California, Santa Barbara, Santa Barbara, CA, United States

[†]Neuroscience Research Institute, University of California, Santa Barbara, Santa Barbara, CA, United States

[‡]Materials Research Laboratory, University of California, Santa Barbara, Santa Barbara, CA, United States

[§]Institute of Chemistry, Hebrew University of Jerusalem, Jerusalem, Israel

[¶]Korea Advanced Institute of Science and Technology, Daejeon, Republic of Korea

[1]Corresponding authors: e-mail address: peterjchung@uchicago.edu; safinya@mrl.ucsb.edu

CHAPTER OUTLINE

[2]Current address: James Franck Institute and Department of Chemistry, University of Chicago, Chicago, Illinois 60,637, United States.
[3]Current address: Amore-Pacific Co. R&D Center, Yongin 446-729, South Korea.

Methods in Cell Biology, Volume 141, ISSN 0091-679X, http://dx.doi.org/10.1016/bs.mcb.2017.06.002

Abstract

Tau, a neuronal protein known to bind to microtubules and thereby regulate microtubule dynamic instability, has been shown recently to not only undergo conformational transitions on the microtubule surface as a function of increasing microtubule coverage density (i.e., with increasing molar ratio of Tau to tubulin dimers) but also to mediate higher-order microtubule architectures, mimicking fascicles of microtubules found in the axon initial segment. These discoveries would not have been possible without fine structure characterization of microtubules, with and without applied osmotic pressure through the use of depletants. Herein, we discuss the two primary techniques used to elucidate the structure, phase behavior, and interactions in microtubule/Tau mixtures: transmission electron microscopy and synchrotron small-angle X-ray scattering. While the former is able to provide striking qualitative images of bundle morphologies and vacancies, the latter provides angstrom-level resolution of bundle structures and allows measurements in the presence of in situ probes, such as osmotic depletants. The presented structural characterization methods have been applied both to equilibrium mixtures, where paclitaxel is used to stabilize microtubules, and also to dissipative nonequilibrium mixtures at 37°C in the presence of GTP and lacking paclitaxel.

1 INTRODUCTION

While the dysfunction of the microtubule-associated protein (MAP) Tau has been linked to numerous neurodegenerative disease (tauopathies), its precise physiological mechanisms of action are not well understood (Ballatore, Lee, & Trojanowski, 2007). This lack of understanding is owing, in large part, to its intrinsically disordered nature; Tau does not form a secondary structure in solution (Schweers, Schönbrunn-Hanebeck, Marx, & Mandelkow, 1994). Tau is thus described by its primary sequence: starting with an N-terminal tail (consisting of the projection domain and proline-rich region), microtubule-binding region, and ending with its C-terminal tail (Lee, Cowan, & Kirschner, 1988).

What is known about Tau is that its microtubule-binding region helps suppress microtubule dynamic instability, where microtubules stochastically alternate between periods of growth (polymerization) and rapid shrinkage (depolymerization) (Drechsel, Hyman, Cobb, & Kirschner, 1992; Goode et al., 1997; Mitchison & Kirschner, 1984; Trinczek, Biernat, Baumann, Mandelkow, & Mandelkow, 1995). However, the regions of Tau that act to regulate dynamic instability compose a relatively small portion of the protein, prompting efforts to understand the other parts of the protein, especially the N-terminal tail of Tau containing the projection domain. The N-terminal tail is differentially expressed into short, medium, and long length projection domains by alternative splicing (Himmler, Drechsel, Kirschner, & Martin, 1989), underscoring a diversity in sequence and, perhaps, an intriguing role in Tau function. The N- and C-terminal regions flanking the microtubule-binding region contain numerous serine-proline and threonine-proline motifs as potential phosphorylation sites for proline-directed kinases with the microtubule-binding region containing a small number of nonproline serine motifs as phosphorylation sites (Dolan & Johnson, 2010). Tau neuropathologies are normally accompanied by abnormal Tau hyperphosphorylation (Augustinack, Schneider, Mandelkow, & Hyman, 2002).

Recently, it has been shown that the N-terminal tail of Tau transitions to a polyelectrolyte brush on the microtubule surfaces as a function of increasing coverage density for the Tau isoforms with longer N-terminal tails (Chung et al., 2015). A conformational change to a polyelectrolyte brush would dramatically increase the steric repulsion of biomacromolecules away from microtubules. However, the N-terminal tail of Tau does not behave as a classic polyelectrolyte brush; in the absence of the microtubule stabilizer paclitaxel, Tau can actually mediate widely spaced bundles of dynamic microtubules through an aggregate of sub-k_BT interactions between Tau proteins on opposing microtubule surfaces (Chung et al., 2016). These bundles in cell-free reconstitutions (in GTP buffer at 37°C) share bundle morphologies strikingly similar to microtubules in both cells with overexpressed Tau and fascicles of microtubules found in the axon initial segment in neurons.

These discoveries would not have been possible without structural characterization techniques such as synchrotron small-angle X-ray scattering (SAXS) and

electron microscopy, the former of which also includes in situ methods that allow for osmotic pressurization of microtubule samples in order to measure tau-mediated forces between microtubules. In this chapter, we will detail the preparation for microtubule and Tau samples for each technique and outline corresponding strengths and weaknesses.

2 GENERAL SAMPLE PREPARATION

As microtubules exhibit dynamic instability, paclitaxel is often used as a stabilizing agent in many biochemical and biophysical assays. The advantage of paclitaxel-stabilized microtubules is experimental tractability; for example, with minimal dynamic instability, microtubules can be used to probe microtubule motors (Kuznetsov & Gelfand, 1986) and other studies looking at the microtubule surface as a substrate.

As opposed to paclitaxel-stabilized microtubules, Tau-stabilized microtubule samples must be assembled immediately prior to measurement or setting (via plastic embedding or cryofixation), as GTP is finite and being continually hydrolyzed by the GTPase tubulin. While Tau does decrease microtubule dynamic instability (especially as a function of increased Tau concentration), it does not eliminate it; time until measurement/setting should be taken into account when preparing samples.

2.1 REAGENTS AND EQUIPMENT NECESSARY FOR GENERAL SAMPLE PREPARATION

For preparation of all aqueous solutions, deionized water (such as ultrapure Milli-Q® water) should be used. All manufacturer and institutional safety procedures should be observed.

1. PEM50: 50 mM PIPES at pH 6.8 (adjusted with ca. 70 mM NaOH), 1 mM $MgCl_2$, and 1 mM EGTA in deionized water. PEM50 will be the primary buffer in which proteins are stored and samples are made, and thus should be vacuum-filtered. EGTA is crucial as EGTA preferentially clathrates Ca^{2+}, which is a known microtubule destabilizer. (Optional: 0.02% NaN_3 may be added for long-term storage and use at room temperature)
2. Tubulin in PEM50: MAP-free tubulin that has been vitrified/drop-frozen in liquid nitrogen of known concentration is necessary and stored at −80°C (Miller & Wilson, 2010)
3. Tau in PEM50 or BRB80 (80 mM PIPES at pH 6.8, 1 mM $MgCl_2$, and 1 mM EGTA in deionized water) and stored at −20°C. Prior to use, Tau should be aliquoted to minimize repeat freeze–thaw cycles; while Tau is an intrinsically disordered protein, cleavage has been noted from multiple freeze–thaw cycles via SDS-PAGE
4. GTP in PEM50 and stored at −20°C. While concentration may vary depending on tubulin/Tau concentrations, a stock solution of 2 mM GTP in PEM50 is usually sufficient

5. *For paclitaxel-stabilized microtubules:* 1 mM Paclitaxel (Cytoskeleton, Inc., Denver, CO) dissolved in DMSO and stored at −20°C
6. *For paclitaxel-stabilized microtubules:* 50% Glycerol dissolved in PEM50 and stored at −20°C
7. Temperature-controlled centrifuge with microcentrifuge tube rotor capable of achieving $10{,}000 \times g$
8. Water bath capable of 37°C

2.2 TAU-INDUCED AND PACLITAXEL-FREE MICROTUBULE BUNDLE SAMPLE PREPARATION

All reagents and samples should be thawed and prepared, respectively, on ice unless otherwise noted. Calculations should be made prior to sample preparation for desired amount of tubulin, Tau/tubulin ratios, and GTP/PEG concentrations. For both EM and SAXS samples, roughly 100 and 200 μg of tubulin is necessary for an observable pellet after centrifugation prior to measurement, respectively.

1. Thaw tubulin on ice. Depending on the volume/concentration/amount of tubulin, this may take 2–4 h.
2. While tubulin is thawing, prechill centrifuge to 4°C (for centrifugation of thawed tubulin) and preheat water bath to 37°C (for microtubule polymerization).
3. Prechill and label individual microcentrifuge tube for each microtubule/Tau sample.
4. Once tubulin has been thawed, centrifuge in prechilled centrifuge at 4°C, $10{,}000 \times g$ for 30 min to separate out soluble tubulin from any possible contaminating aggregates.
5. After centrifugation, prewarm centrifuge to 37°C for centrifugation of electron microscopy/SAXS samples.
6. Dispense necessary amounts of tubulin into appropriate and labeled sample tubes.
7. Dispense necessary amounts of Tau into appropriate and labeled sample tubes, slowly mixing while pipetting into sample solution. Take care to avoid introducing bubbles in solution; increase in air/solution interfaces alters the polymerization dynamics of microtubules.
8. Dispense necessary amounts of GTP into appropriate and labeled sample tubes, slowly mixing while pipetting into sample solution.
9. When all samples have been prepared, place in water bath set at 37°C for 40 min. Sample tubes should be placed in Teflon "floaters" to stabilize tubes. After this point, take care to minimize the amount of time samples spend outside of 37°C.

At this point, Tau-induced microtubule bundles have formed within solution (provided there is sufficient Tau and GTP) but as GTP is continuously being depleted, it is critical that samples be either measured or set quickly. Preparation of samples for each particular characterization technique will vary.

2.3 PACLITAXEL-STABILIZED AND TAU-COATED MICROTUBULE SAMPLE PREPARATION

All reagents and samples should be thawed and prepared, respectively, on ice unless otherwise noted. Calculations should be made prior to sample preparation for desired amount of tubulin, Tau/tubulin ratios, and GTP/PEG/paclitaxel concentrations. (Note: While our paclitaxel-stabilized microtubules were assembled at a paclitaxel:tubulin ratio of 1:1, decreasing the amount of paclitaxel will slowly increase Tau-mediated bundle formation (Choi et al., 2017).) For both EM and SAXS samples, roughly 100 and 200 μg of tubulin is necessary for an observable pellet after centrifugation, respectively.

1. Thaw tubulin on ice. Depending on the concentration/amount of tubulin, this may take 2–4 h.
2. While tubulin is thawing, prechill centrifuge to 4°C (for centrifugation of thawed tubulin) and preheat water bath to 37°C (for microtubule polymerization).
3. Prechill and label individual microcentrifuge tube for each microtubule/Tau sample.
4. Once tubulin has been thawed, centrifuge in prechilled centrifuge at 4°C, $10{,}000 \times g$ for 30 min to separate out soluble tubulin from any possible contaminating aggregates.
5. After centrifugation, prewarm centrifuge to 37°C for centrifugation of electron microscopy/SAXS samples.
6. Dispense necessary amounts of tubulin into appropriate and labeled sample tubes.
7. Dispense necessary amounts of GTP into appropriate and labeled sample tubes, slowly mixing while pipetting into sample solution.
8. Dispense necessary amount of 50% glycerol stock solution to get each sample to 5% overall glycerol concentration.
9. Dispense necessary amounts of paclitaxel into appropriate and labeled sample tubes, slowly mixing while pipetting into sample solution. As paclitaxel is suspended in DMSO, mixing must be done thoroughly (for ~1 min per sample).
10. When all samples have been prepared, place in water bath set at 37°C for 40 min. Sample tubes should be placed in Teflon "floaters" to stabilize tubes. After this point, take care to minimize time samples spend outside of 37°C.
11. Dispense necessary amounts of Tau into appropriate and labeled sample tubes after polymerization, slowly mixing while pipetting into sample solution. Take care to avoid introducing bubbles in solution; while microtubules should be stable, bubbles make later pipetting difficult.

At this point, paclitaxel-stabilized and Tau-coated microtubules have formed within solution. Due to paclitaxel stabilization, samples will be stable for up to 1 week, allowing large-scale preparation before a particular characterization technique.

3 DIFFERENTIAL INTERFERENCE CONTRAST MICROSCOPY

Differential interference contrast (DIC) microscopy is a relatively low-resolution optical microscopy technique that allows imaging of unstained and transparent samples by giving the perception of depth by having regions with longer optical paths appear darker, while shorter optical paths appear lighter. It is generally considered a good first step to assess whether microtubules and/or microtubule bundles have formed (Fig. 1).

3.1 REAGENTS AND EQUIPMENT NECESSARY FOR DIC MICROSCOPY SAMPLE PREPARATION

For preparation of all aqueous solutions, deionized water (such as ultrapure Milli-Q® water) should be used. All manufacturer and institutional safety procedures should be observed.

1. *For Tau-mediated microtubule bundle samples:* Temperature-controlled sample stage for slide mount. Usually, this must be custom designed or bought per DIC microscope specifications
2. Microscope slide
3. Microscope cover slip (size smaller than that of the microscope slide)
4. Wax or fast-setting epoxy (in particular, Devcon® 5 Minute Epoxy seems to work well)

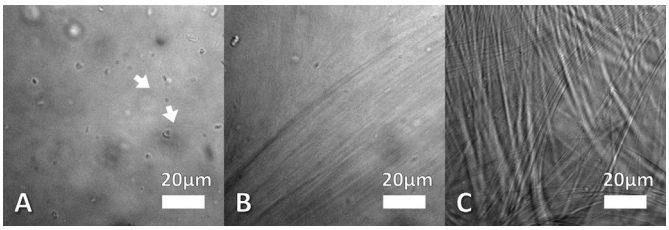

FIG. 1

Tau mediates microtubules into bundling at 37°C in 2 mM GTP with and without centrifugation, demonstrating phase separation induced by Tau-mediated attractions between microtubules. (A) While individual microtubules (*arrows*) can be identified via differential interference contrast (DIC) microscopy, no discernible bundles have formed in paclitaxel-free microtubules without Tau. (B) Without centrifugation, microtubules form clear bundles when assembled with Tau, demonstrating an attractive component of the Tau-mediated microtubule–microtubule interaction. (C) With centrifugation (10,000 × *g* for 30 min at 37°C), increased density of bundles assembled with Tau is observed. Scale bars, 20 μm.

3.2 SAMPLE PREPARATION FOR DIC MICROSCOPY

1. You can either decide to image centrifuged or noncentrifuged samples, with the former providing much higher microtubule density. For centrifuged samples, samples should be centrifuged at 37°C, 10,000 × *g* for 30 min to form a microtubule pellet.
2. Pipette 3–10 μL of a nonpelleted (solution) or pelleted sample from your sample tube directly onto your sample slide.
3. Place the microscope cover slip over the slide.
4. Seal the cover slip with wax or fast-setting epoxy.
5. For Tau-mediated microtubule bundle samples, place slide with sample onto the temperature-controlled sample stage. For paclitaxel-stabilized microtubule samples, place slide with sample onto sample stage.

4 TRANSMISSION ELECTRON MICROSCOPY

Electron microscopy is a robust characterization method of Tau-induced microtubule bundles, but care must be taken as setting/fixation may alter the microtubule bundle morphologies.

For sample preparation by whole mount, samples are dehydrated on an electron microscopy grid. While this preparation maintains bundles in microtubule samples, quantitative information of intermicrotubule spacing cannot be assessed due to the dehydration. This characterization and sample preparation is optimal as a "quick check" for microtubule bundling.

Plastic embedding is a transmission electron microscopy (TEM) sample preparation by which Tau-mediated microtubule bundles will be "locked" into place via a polymer matrix, with the added benefit of allowing characterization by examining bundles both along the longitudinal axis and in cross section (Fig. 2). However, as water is initially replaced with acetone in this preparation, plastic embedding offers a good qualitative description of microtubule bundles while lacking the quantitative accuracy of other in situ techniques.

As opposed to whole-mount sample preparation, plastic embedding is an involved process requiring recent reagent preparation and a clear timetable for samples to be prepared. In this section, we will be outlining a 3-day preparation technique: sample fixation, sample dehydration and plastic infiltration, and plastic templating.

4.1 WHOLE-MOUNT SAMPLES FOR TEM

4.1.1 Reagents and equipment necessary for whole-mount sample preparation

For preparation of all aqueous solutions, deionized water (such as ultrapure Milli-Q® water) should be used. All manufacturer and institutional safety procedures should be observed, especially for uranyl acetate.

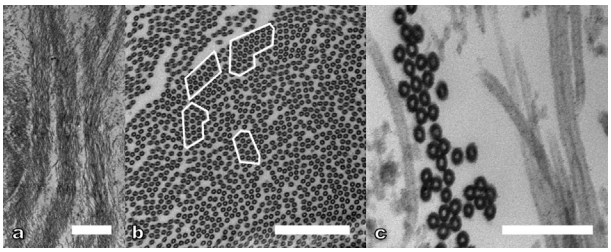

FIG. 2

Plastic-embedded sample preparations reveal microtubule bundles through electron microscopy, in widely spaced and close-packed geometries. (A) Tau-mediated bundles show distinct bundled domains of microtubules. (B) Plastic-embedded Tau-mediated microtubule bundles reveal domains exhibiting hexagonal lattice symmetry. (C) Truncation of the anionic component of the N-terminal tail of Tau brings about close-packed microtubules, as seen through plastic-embedded samples. Scale bars, 1 μm (A), 500 nm (B), and 150 nm (C).

Adapted from Chung, P. J., Song, C., Deek, J., Miller, H. P., Li, Y., Choi, M. C., et al. (2016). Tau mediates microtubule bundle architectures mimicking fascicles of microtubules found in the axon initial segment. Nature Communications, 7, *12278. Retrieved from http://dx.doi.org/10.1038/ncomms12278 and reprinted by permission from Macmillan Publishers Ltd. ©2016.*

1. PEM50: 50 mM PIPES at pH 6.8, 1 mM $MgCl_2$, and 1 mM EGTA in deionized water
2. Formvar-coated copper grids suitable for TEM
3. Filter paper for wicking solution off copper grids
4. Inverted tweezers for handling filter paper/EM grids
5. 1 w/v% of uranyl acetate in deionized water for staining of samples

4.1.2 Whole-mount sample preparation for TEM

1. Desired samples should be centrifuged at 37°C, 10,000 × *g* for 30 min to form a microtubule bundle pellet.
2. After discarding supernatant from each sample tube, the pellet should be diluted with 250 μL of buffer (PEM50), gently pipetting up and down to break apart the pellet into low- and high-density regions.
3. Using two pairs of inverted tweezers, grip a copper grid with one pair and precut filter paper with the other.
4. Pipette 10 μL of a low-density region onto a copper grid, letting the solution sit on the copper grid for 2 min.
5. After 2 min, use filter paper to wick off the sample solution. Gently touch the edge of the copper grid with the filter paper perpendicular to the face of the grid. You may need to tilt the filter paper toward the sample slightly. (Note: while wicking, be sure to wait for the grid to be completely free of solution. You will

notice a quick initial absorption of solution, then a slower pulling of a liquid film from the grid surface. Apply continuous, even pressure until all the liquid is gone).

6. Pipette 10 μL of 1% uranyl acetate solution (1 w/v% of uranyl acetate in deionized water) onto the grid. Let it sit for 20 s and wick the solution off with a fresh filter paper as before.
7. Let the grids dry out overnight before imaging with TEM.

4.2 PLASTIC-EMBEDDED SAMPLES FOR TEM

4.2.1 Reagents and equipment for day 1: Sample fixation

For preparation of all aqueous solutions, deionized water (such as ultrapure Milli-Q® water) should be used. All manufacturer and institutional safety procedures should be observed; this is especially relevant as many components of plastic embedding process are carcinogenic. Specifically, uranyl acetate solution should be performed under a fume hood.

1. 8 w/v% of aqueous glutaraldehyde in deionized water (Sigma-Aldrich, St. Louis, MO)
2. Tannic acid
3. PEM50: 50 mM PIPES at pH 6.8, 1 mM $MgCl_2$, and 1 mM EGTA in deionized water
4. Pelleted sample in 1.5 mL microcentrifuge tube
5. *In preparation for day 2:* "Spurr" Low Viscosity Kits (Ted Pella, Redding, CA). These kits consist of ERL-4221 solution and DER® 736, NSA, and DMAE compounds necessary for plastic infiltration
6. *In preparation for day 2:* 50 mL of 100% acetone
7. *In preparation for day 2:* PolyCut-Ease (Polysciences Inc., Warrington, PA), which will be added to the plastic resin to make microtome sectioning easier

4.2.2 Plastic embedding sample preparation for day 1: Sample fixation

1. Dilute 1 mL of fresh 8 w/v% aqueous glutaraldehyde using 3 mL of PEM50 to obtain 4 mL of fresh 2.0 w/v% glutaraldehyde solution. At alkaline pH values, glutaraldehyde can polymerize by aldol condensation, yielding alpha, beta-unsaturated polyglutaraldehyde. This reaction is minimized by making a fresh and dilute solution of glutaraldehyde.
2. Add 0.06 g of tannic acid to the 4 mL of 2.0 w/v% glutaraldehyde solution and mix thoroughly to obtain a 4.0 w/v% tannic acid in 2.0 w/v% glutaraldehyde solution.
3. Add 1.3 mL of tannic acid/glutaraldehyde solution to the sample pellet and cap the tube.
4. Let sample sit for 7 h at room temperature to allow for the reaction to occur.
5. *For preparation of plastic mixtures from "Spurr" Low Viscosity Kits:* Add the following components, in turn, to a beaker. All components should be weighed,

as gravimetric measurements are more accurate than volumetric measurements for viscous solutions.
   a. 5.0 g of ERL-4221 solution
   b. 4.0 g of DER compound
   c. 13.0 g of NSA compound
6. Stir plastic mixture steadily but not quickly via a low-velocity shaker for $\geq$2 h, while keeping the beaker covered with parafilm. This is to avoid introducing air bubbles.
7. Add 0.2 g of PolyCut-Ease to the plastic mixture and mix again, again avoiding introducing air bubbles.
8. Add 0.2 g of DMAE to the plastic mixture and stir again; this mixture should be deposited into a tube labeled "100% plastic."
9. In a new tube labeled "33.3% plastic," transfer 4 mL of 100% plastic mixture and dilute it with 8 mL of acetone, mixing thoroughly by slowly inverting the tubes 10–15 times.
10. In a new tube labeled "66.6% plastic," transfer 8 mL of 100% plastic mixture and dilute it with 4 mL of acetone, mixing thoroughly by slowly inverting the tubes 10–15 times.

4.2.3 Reagents and equipment for day 2: Sample dehydration and plastic infiltration

For preparation of all aqueous solutions, deionized water (such as ultrapure Milli-Q® water) should be used. All manufacturer and institutional safety procedures should be observed.

1. 3.0 mL of PEM50 per sample
2. 1.3 mL of 0.8 w/v% osmium tetroxide solution (ACROS Organics, Morris Plains, NJ) in PEM50 per sample
3. 1.3 mL of 1.0 w/v% uranyl acetate in DI water per sample
4. 6.0 mL of PEM50 buffer per sample
5. 6.0 mL of DI water per sample
6. 1.0 mL of 25% acetone in DI water per sample
7. 1.0 mL of 50% acetone in DI water per sample
8. 1.0 mL of 75% acetone in DI water per sample
9. 1.0 mL of 100% acetone per sample
10. "100% plastic" mixture made on day 1
11. "66.6% plastic" mixture made on day 1
12. "33.3% plastic" mixture made on day 1

4.2.4 Plastic embedding sample preparation for day 2: Sample dehydration and plastic infiltration

1. Decant the tannic acid/glutaraldehyde solution from the microcentrifuge tube with the now fixed pellet.

2. Add 1.0 mL of PEM50 to the pellet and gently pipette up and down a few times, taking care to avoid dislodging the pellet.
3. Remove PEM50 buffer, repeat steps 2 and 3 twice.
4. Add 1.3 mL of 0.8 w/v% osmium tetroxide solution to the now fixed pellet and cap the tube.
5. Wait more than 1 h (the pellet should start to look dark).
6. Add 1.0 mL of PEM50 to the now fixed and stained pellet and gently pipette up and down a few times.
7. Remove PEM50 buffer, repeat steps 6 and 7 three times to remove osmium tetroxide.
8. Add 1.3 mL of 1.0 w/v% uranyl acetate solution to the now fixed and stained pellet and cap the tube.
9. Wait 1 h.
10. Remove the uranyl acetate solution.
11. Add 1.0 mL of DI water to the now fixed and stained pellet and gently pipette up and down a few times.
12. Remove DI water, repeat steps 11 and 12 three times.
13. To begin dehydration of the fixed and stained pellet, add 1.0 mL of 25% acetone solution to the tube and cap it.
14. Wait 15 min and then decant the 25% solution from the tube.
15. Add 1.0 mL of 50% acetone solution to the tube and cap it.
16. Wait 15 min and then decant the 50% solution from the tube.
17. Add 1.0 mL of 75% acetone solution to the tube and cap it.
18. Wait 15 min and then decant the 75% solution from the tube.
19. Add 1.0 mL of 100% acetone solution to the tube and cap it.
20. Wait 15 min and then decant the 100% solution from the tube.
21. Repeat steps 19 and 20 three more times.
22. Add 1.3 mL of "33.3% plastic" to the tube and cap it to begin plastic infiltration.
23. Set the tube on a shaker for 1 h and decant "33.3% plastic" solution.
24. Add 1.3 mL of "66.6% plastic" to the tube and cap it.
25. Set the tube on a shaker for 1 h and decant "66.6% plastic" solution.
26. Add 1.3 mL of "100% plastic" to the tube and cap it.
27. Set the tube on a shaker for 1 h and decant "100% plastic" solution.
28. Add another 1.3 mL of "100% plastic solution" to the tube and cap it.
29. Set the tube to shake overnight.

4.2.5 Reagents and equipment for day 3: Plastic templating

For preparation of all aqueous solutions, deionized water (such as ultrapure Milli-Q® water) should be used. All manufacturer and institutional safety procedures should be observed.

1. 1.0 mL of "100% plastic" mixture
2. Sample labels written with lead pencil (ink contains an organic solvent that will dissolve in the plastic mixture and most likely render the label illegible)

3. Sample template (Ted Pella, Redding, CA)
4. Oven capable of reaching 65°C
5. Microtome

4.2.6 Plastic embedding sample preparation for TEM

1. Aliquot a small volume of "100% plastic" mixture into each of the template grooves and insert sample labels.
2. Decant each sample mixture from the overnight shake into an appropriate template groove with sample label.
3. Gently scrape the sample pellet off the bottom of the sample tube and make sure it is placed within each respective labeled template groove. Position the sample pellet as close to the end of the sample template as possible such that the pellet remains coated on all sides by the plastic mixture.
4. After the sample is placed into its groove, fill the rest of the groove with the "100% plastic" mixture.
5. After preparing all samples, place the template in a 65°C and let them set for 48 h.
6. Allow the plastic samples to cool overnight before microtoming.

4.2.7 Trimming of the specimen block

1. Cut the sample block roughly with Razor. The foreface of the trapezoid must be the black-colored part.
2. Position the sample block on the sample block on the sample arm.
3. Mount the glass knife and put some water into the knife trough. Turn the microtome control on.
4. Start making larger sections with the thickness 1 μm until the sectioning surface is smooth and uniform.
5. Change the glass knife to the diamond knife and then begin making the thinner sample sections with about 50 nm thickness.
6. To collect the desirable section, grab the carbon grid and place it into the water at an angle beneath the section of choice and then lift upward. Waving a cotton swab wet with chloroform over the sections floating on the water will make them to unwrinkle.
7. Holding the grid with the section and touch the edge of the grid with the filter paper perpendicular to the face of the grid.
8. Let the grids dry out overnight before imaging with TEM.

5 SYNCHROTRON SMALL-ANGLE X-RAY SCATTERING

SAXS is a powerful method for obtaining angstrom-level resolution of ordered assemblies in solution, allowing not only precise quantitative measurements of bundle assemblies but also allowing for varying of solution conditions, including (but not limited to) changes in temperature, salt, pH, and osmotic pressure. While most biological assemblies are carefully tuned for both temperature and pH, exploring the

changes to structure as a function of salt and osmotic pressure allow for measurement of forces that would otherwise be impossible using other techniques.

However, SAXS also has limitations. SAXS is an ensemble-averaging technique, which emphasizes denser, more highly ordered regions at the expense of less dense, more disordered regions. Furthermore, SAXS is usually reliant on an accurate and representative model to fit reciprocal space data, requiring a complementary real-space technique (like electron microscopy).

5.1 REAGENTS AND EQUIPMENT NECESSARY FOR SAXS SAMPLE PREPARATION

For preparation of all aqueous solutions, deionized water (such as ultrapure Milli-Q® water) should be used. All manufacturer and institutional safety procedures should be observed.

1. Quartz capillaries for SAXS measurements. For our purposes, we used 1.5 mm diameter/ 0.01 mm wall thickness quartz capillaries with funnels for sample loading (Hilgenberg GmbH, Malsfeld, Germany).
2. Cutting stone or diamond knife suitable for etching quartz capillaries.
3. A temperature-controlled centrifuge designed for capillary centrifugation. For our purposes, we used a Universal 320R centrifuge with a 2076 hematocrit rotor (Hettich, Tuttlingen, Germany).
4. A quick setting epoxy.
5. An oven designed to maintain samples at 37°C with X-ray transparent windows. Usually, this must be custom designed and built per X-ray source specifications.
6. (For osmotic pressure sample measurements only) Poly(ethylene glycol) (PEG) of appropriate molecular mass (see Section 5.4.1) in PEM50.
7. (For osmotic pressure sample measurements only) Narrow gel-loading pipette tips that are sufficiently narrow to fit inside the capillary.

5.2 SAXS SAMPLE PREPARATION

Although time spent at temperatures lower than 37°C is unavoidable, once microtubule bundles have been prepared such time should be minimized to protect against cold-induced depolymerization of microtubules.

1. Desired samples should be loaded into individual quartz capillaries. Samples can be initially pushed to the bottom of the capillary using a strong flick of the wrist, taking care to avoid crushing the capillary or letting it go.
2. Prior to placement into capillary rotor, capillary funnels should be removed using a cutting stone or diamond knife.
3. Samples in quartz capillaries should be centrifuged at 37°C, $10{,}000 \times g$ for 30 min to form a microtubule bundle pellet with density suitable for X-ray scattering.

4. (For osmotic pressure sample measurements only) Appropriate amount of PEG solution should be added to the capillary with a gel-loading pipette tip and pushed to the top of the solution within the centrifuged capillary with strong flicks of the wrist. PEG solution must be added after centrifugation; otherwise, samples may be possibly sheared during the centrifugation process.
5. The top of each capillary should be sealed with epoxy.
6. Each sample should be loaded into the oven, which will be subsequently mounted onto the sample stage for X-ray measurements.

Although specifications for X-ray sources may vary, synchrotron radiation is optimal for both minimizing time required for data measurement and maximizing quality of data, especially at a beamline engineered for SAXS. Our data were taken at Stanford Synchrotron Radiation Lightsource (SLAC National Accelerator Laboratory, Palo Alto, CA) beamline 4-2 with a 9 keV beam with Si(111) monochromator. Scattering data were acquired with a 2D area detector (MarUSA, Evanston, IL).

5.3 SAXS DATA ANALYSIS

While data analysis of SAXS data may seem formidable at first, as long as one has a good understanding of the shape of the scattering object (form factor) and lattice geometry (structure factor), it is fairly straightforward as long as one has a background with at least one programming language (MATLAB is particularly suited for SAXS data analysis). As we are working with microtubules that bundle (with and without osmotic pressure), the form factor and structure factor we will be focusing on are hollow cylinders and hexagonal lattices, respectively (Fig. 3). However, there are more theoretical and encompassing perspectives (Cullity, 1957; Glatter & Kratky, 1982; Warren, 1990) on X-ray scattering available.

5.3.1 The form factor of microtubules

Microtubules have been modeled (with great success) as hollow cylinders of constant charge density in interpreting X-ray scattering data (Andreu et al., 1992; Choi et al., 2011, 2009; Chung et al., 2015, 2016; Needleman et al., 2005, 2013; Needleman, Ojeda-Lopez, Raviv, Ewert, et al., 2004; Needleman, Ojeda-Lopez, Raviv, Miller, et al., 2004; Ojeda-Lopez et al., 2014; Raviv et al., 2005, 2007, Safinya et al., 2011, 2016), especially at the angles at which the microtubule form factor is relevant. For a given hollow cylinder with inner radius r_{in}, shell thickness δ, and cylinder length $2H$, the form factor is:

$$f(Q_\perp, Q_z) = \rho_0 \int_{-H}^{H} e^{-iQ_z \cdot z} dz \int_{r_{\text{in}}}^{r_{\text{in}}+\delta} \rho d\rho \int_{0}^{2\pi} e^{-iQ_\perp \cdot \rho \cos\theta} d\theta$$

which simplifies to:

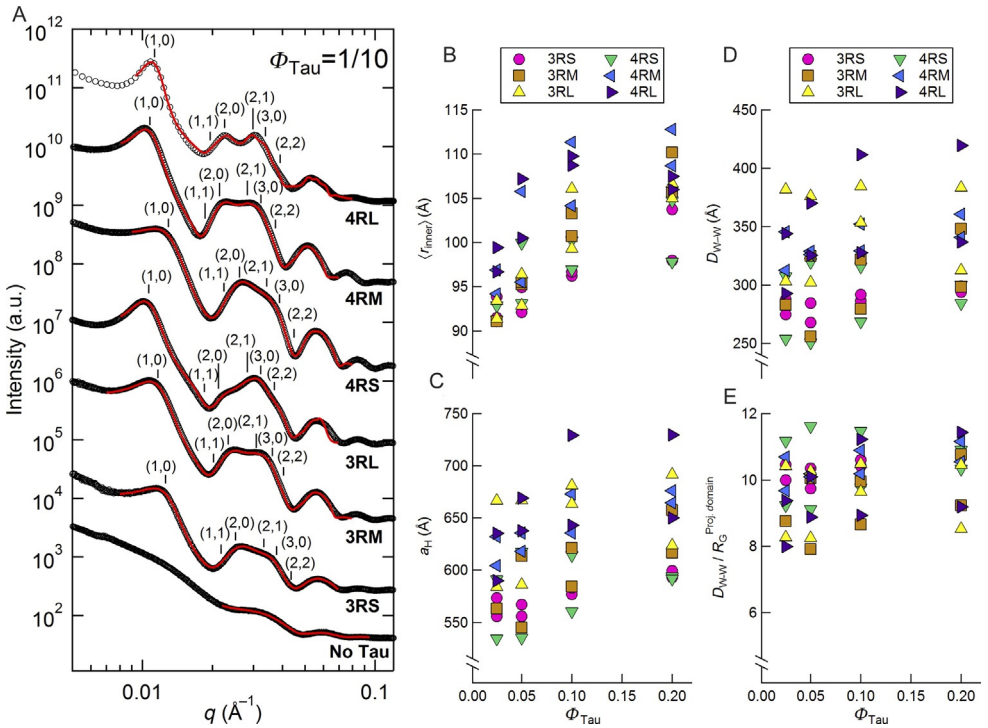

FIG. 3

An example of data and extracted parameters from SAXS data analysis. (A) X-Ray line shapes for Tau-mediated microtubule bundles for all six Tau wild-type isoforms (*top six line shapes*), compared to microtubules without Tau (*bottom line shape*), with fits in *red*. In these SAXS studies no paclitaxel was used and microtubules were stabilized with Tau at 37°C in the presence of 2 mM GTP. (B–E) With SAXS data analysis, it is possible to extract the inner radii of microtubules as a function of increasing Tau concentration (B), the hexagonal lattice parameters (C), the wall-to-wall distance between microtubules (D), and the wall-to-wall distance normalized by the expected radius of gyration for a disordered peptide with length equal to the projection domain.

$$f(Q_\perp, Q_z) = \frac{2\pi\rho_0 J_0(Q_z H)}{Q_\perp}[(r_{\text{in}} + \delta) * J_1(Q_\perp(r_{\text{in}} + \delta)) - r_{\text{in}} * J_1(Q_\perp r_{\text{in}})]$$

where J_0 and J_1 correspond to Bessel functions of the first kind of order zero and one, respectively. Thus, the predicted scattering intensity is the product of the form factor with its complex conjugate:

$$I(\mathbf{Q}) = ff^* = \left(\frac{2\pi\rho_0 J_0(Q_z H)}{Q_\perp}[(r_{\text{in}} + \delta) * J_1(Q_\perp(r_{\text{in}} + \delta)) - r_{\text{in}} * J_1(Q_\perp r_{\text{in}})]\right)^2$$

However, this would correspond to the scattering of a single microtubule, not many microtubules simultaneously. As the microtubules are in solution and are thus free to take any and all orientations, the predicted scattering of a microtubule must be orientationally averaged to account for all possible microtubule orientations:

$$I(Q) = \langle I(\mathbf{Q})\rangle_{\text{Orient.}} = \frac{1}{4\pi}\int_0^{\pi}\int_0^{2\pi} I(\mathbf{Q})\sin\theta d\theta d\phi$$

These equations should underscore the need for numerical integration provided by most programming platforms.

While the aforementioned model is suitable under the assumption of simplifying geometry (i.e., a microtubule as a hollow cylinder of constant charge density), it has been recently shown to be possible to calculate the expected scattering from microtubules by calculating the scattering amplitude of tubulin subunits "meshed" over a grid in reciprocal space (Ginsburg et al., 2016). This method can be used to examine the precise arrangement of individual tubulin in microtubules over a wide range of scattering angles.

5.3.2 The structure factor of microtubules

While the form factor mathematically describes the expected scattering of an object, the structure describes the expected scattering (as a result of constructive/destructive interference) off of a lattice of objects. Fitting both structure factor and form factor is simplified through the *convolution theorem*, which allows one to simply take the product of the structure and form factor for the expected result.

For the purposes of microtubule bundles, we found them to be either in a rectangular lattice symmetry or hexagonal symmetry, the latter always the case with Tau-mediated microtubule bundles. We empirically found the structure factor peaks associated with microtubules are best fit with squared Lorentzians with peak amplitudes A_{hk} and peak width κ_{hk}:

$$S(q_\perp) = \sum_{h,k=0}^{h,k}\left(\frac{A_{hk}}{\left(\kappa_{hk}{}^2 + (q_\perp - G_{hk})^2\right)}\right)^2$$

where G_{hk} is dependent on the lattice geometry. For hexagonal lattices:

$$|G_{hk}| = q_{10}\sqrt{h^2 + k^2 + hk^2}$$

where q_{10} is the first observed structure factor peak.

5.4 SAXS OSMOTIC PRESSURE SAMPLES

One of the unique advantages of in situ sample measurements is the ability to add noninteracting polymeric depletants to samples to induce osmotic pressure between colloidal objects (in our case, microtubules) (Fig. 4). As the force applied can be calculated via osmotic depletants added and the change in distance between microtubules measured by SAXS analysis, a force–distance diagram can be obtained. This reveals valuable information with regard to the nature and magnitude of interactions between microtubules while also replicating the macromolecular crowded conditions of the cell.

Briefly, this "depletion force" is an attractive, entropic force between large colloidal particles as a result of being suspended in a dilute solution of smaller solutes or depletants (Asakura & Oosawa, 1958). Often, depletants are preferentially excluded near the vicinity of colloidal particles owing to an entropically favorable reduction in the colloidal excluded volume, causing the colloids to "attract" as a function of colloidal geometry, depletant size, and depletant concentration. While this technique was first used in biological reconstitutions to measure the forces between lipid bilayers (Parsegian, Fuller, & Rand, 1979) and DNA macroions (Parsegian, Rand, Fuller, & Rau, 1986), it has been extended to measure the forces between elements in cytoskeletal networks, such as neurofilaments (Beck, Deek, Jones, & Safinya, 2010; Deek, Chung, Kayser, Bausch, & Safinya, 2013; Safinya, Deek, Beck, Jones, & Li, 2015) and microtubules (Chung et al., 2015, 2016; Needleman, Ojeda-Lopez, Raviv, Ewert, et al., 2004).

5.4.1 Choice of depletant

The osmotic pressure that can be effected by the depletant will depend on the following variables, some of which must be evaluated in tandem:

1. The depletant should not directly interact with the colloids being depleted; thus, the choice of PEG/PEO as the depletant of choice for many systems as it is considered to be biologically inert. (As an aside, poly(ethylene glycol), or PEG, and poly(ethylene oxide), or PEO, are chemically equivalent, but PEG is usually used for polymers with molecular mass $\leq$20,000 Da, while PEO is used for polymers with molecular mass $>$20,000 Da). Should the depletant have known direct interactions with the colloid, a semi-permeable membrane is required (physically segregating colloids and depletants), which is technically challenging for capillary samples.

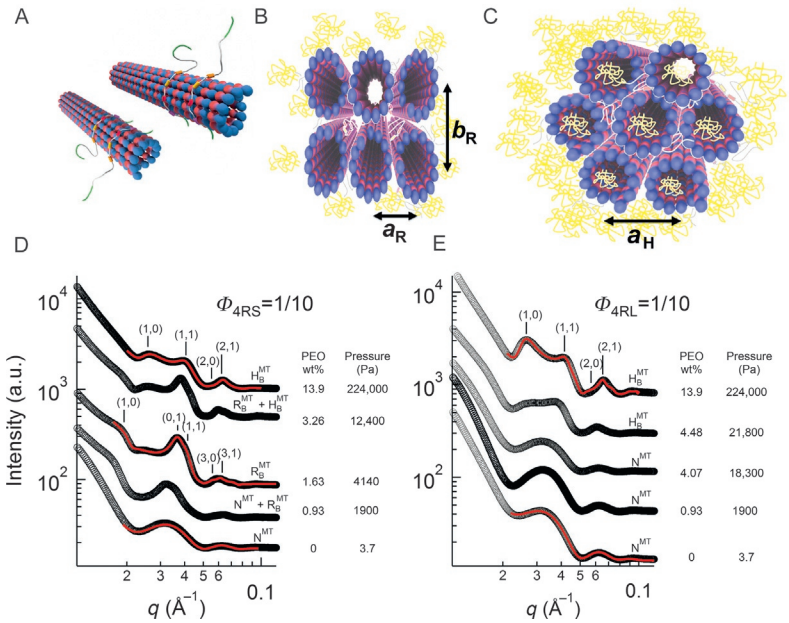

FIG. 4

Paclitaxel-stabilized microtubules with Tau may still be bundled under the influence of osmotic pressure, with structure deducible via the SAXS. (A–C) While paclitaxel-stabilized microtubules do not have a higher-order structure and are, instead, nematically aligned (A), under osmotic pressure microtubules can transition to a buckled rectangular phase (B) and a hexagonal phase (C). (D,E) While microtubules coated with Tau isoforms with the shortest projection domain (4RS Tau to tubulin ratio, $\Phi_{4RS} = 1/10$) exhibit a standard transition from nematic to buckled rectangular to hexagonally bundled microtubules, microtubules coated with Tau isoforms with the longest projection domain (4RL Tau to tubulin ratio $\Phi_{4RL} = 1/10$) require a much higher osmotic pressure for the columnar phase to begin and, even then, only exhibit the hexagonally bundled phase.

Adapted from Chung, P. J., Choi, M. C., Miller, H. P., Feinstein, H. E., Raviv, U., Li, Y., et al. (2015). Direct force measurements reveal protein Tau confers short-range attractions and isoform-dependent steric stabilization to microtubules. Proceedings of the National Academy of Sciences of the United States of America, 112*(47), E6416–E6425.* http://dx.doi.org/10.1073/pnas.1513172112.

2. The size of the depletant should be equal to or larger than the intercolloidal distances being probed. Tau-mediated microtubule bundles can have intermicrotubule spacings of ~40 nm, requiring depletants equal to or larger than ~40 nm for direct force measurements. Prior work (Devanand & Selser, 1991) measured the radius of gyration (R_G) as a function of PEG molecular mass (MW):

$$R_G = 0.215\mathrm{MW}^{0.583}$$

The effective depletant radius (a) can be thus calculated:

$$a = \frac{2R_G}{\sqrt{\pi}}$$

3. The prior variable must be balanced against the desired osmotic pressure range to be probed. Normally, smaller depletants (e.g., PEG with lower molecular masses) are ideal for probing higher osmotic pressures as an equivalent w/v% of a lower molecular mass PEG means higher number density of PEG molecules can be achieved, thus increasing the dynamic range of the depletion force. However, if the depletant is not sufficiently large, the depletant will penetrate the intercolloidal space and result in inaccurate force–distance measurements.
4. Prior osmotic pressure characterization of the depletant chosen is ideal, especially at the desired temperature. It is also possible to calculate the osmotic pressure effect of the depletant, without prior characterization, as a virial expansion with theoretical/calculated virial coefficients, but direct experimental observation is preferred.

5.4.2 Calculating osmotic pressure from depletant concentration

Sometimes (but not often!) the amount of depletant solution will make the overall depletant concentration match a prior measurement. For example, suppose that 10 μL of 25 w/v% stock solution of PEG8k has been added to 40 μL of sample solution set to 35°C. According to available osmotic pressure data (Stanley & Strey, 2003), this 5 w/v% solution of PEG8k (overall) has the equivalent osmotic pressure of 37,800 Pa.

However, one is not usually so fortunate. The oft-used strategy for an arbitrary w/v% is to fit available data at one temperature across multiple concentrations of corresponding depletant, with either a modified exponential fit (Rand, n.d.) or a power law fit (Cohen & Highsmith, 1997), the latter based on the mathematical form of the virial expansion. As long as the desired osmotic pressure for a desired w/v% is within the limits of reported data, either fit performs adequately.

In the case that direct osmotic pressure data are not available, the problem becomes slightly more difficult. As there is more literature available on the second virial coefficient of aqueous solutions of various depletants, it is quite possible to theoretically derive the osmotic pressure on the basis of number concentration alone. We have found that this derivation is reasonable as long as the overall depletant concentration is within the dilute limit (i.e., below the overlap concentration, c^*).

ACKNOWLEDGMENTS

Research primarily supported by the US Department of Energy (DOE), Office of Science, Basic Energy Sciences (BES) under award number DE-FG02-06ER46314 (self-assembly and force measurements in filamentous protein systems), the US National Science Foundation (NSF) under award number DMR-1401784 (protein phase behavior), and the US National

Institutes of Health under award numbers R01-NS13560 and R01-NS35010 (tubulin purification and protein Tau isoform purification from plasmid preparations). U.R. acknowledges support from the Israel Science Foundation (Grant 656/17). M.C.C. was supported by NRF-2014R1A1A2A16055715, 2014M2B2A4030706, and APCTP. The x-ray diffraction work was carried out at the Stanford Synchrotron Radiation Lightsource, a Directorate of SLAC National Accelerator Laboratory and an Office of Science User Facility operated for the US DOE Office of Science by Stanford University. The SSRL Structural Molecular Biology Program which supports BL4-2 is funded by the DOE Biological and Environmental Research and the NIH National Institute of General Medical Science (P41GM103393).

REFERENCES

Andreu, J. M., Bordas, J., Diaz, J. F., de Ancos, J. G., Gil, R., Medrano, F. J., et al. (1992). Low resolution structure of microtubules in solution. *Journal of Molecular Biology*, *226*(1), 169–184. http://dx.doi.org/10.1016/0022-2836(92)90132-4.

Asakura, S., & Oosawa, F. (1958). Interaction between particles suspended in solutions of macromolecules. *Journal of Polymer Science*, *33*(126), 183–192. http://dx.doi.org/10.1002/pol.1958.1203312618.

Augustinack, J. C., Schneider, A., Mandelkow, E. M., & Hyman, B. T. (2002). Specific tau phosphorylation sites correlate with severity of neuronal cytopathology in Alzheimer's disease. *Acta Neuropathologica*, *103*(1), 26–35. http://dx.doi.org/10.1007/s004010100423.

Ballatore, C., Lee, V. M.-Y., & Trojanowski, J. Q. (2007). Tau-mediated neurodegeneration in Alzheimer's disease and related disorders. *Nature Reviews Neuroscience*, *8*(9), 663–672. http://dx.doi.org/10.1038/nrn2194.

Beck, R., Deek, J., Jones, J. B., & Safinya, C. R. (2010). Gel-expanded to gel-condensed transition in neurofilament networks revealed by direct force measurements. *Nature Materials*, *9*(1), 40–46. http://dx.doi.org/10.1038/nmat2566.

Choi, M. C., Chung, P. J., Song, C., Miller, H. P., Kiris, E., Li, Y., et al. (2017). Paclitaxel suppresses tau-mediated microtubule bundling in a concentration-dependent manner. *Biochimica et Biophysica Acta: General Subjects*, *1861*, 3456–3463.

Choi, M. C., Raviv, U., Li, Y., Miller, H. P., Needleman, D. J., Kim, M. W., et al. (2011). Synchrotron small angle x-ray scattering quantitatively detects angstrom level changes in the average radius of taxol-stabilized microtubules decorated with the microtubule-associated-protein tau. *Journal of Physics: Conference Series*, *272*(1), 12001. http://dx.doi.org/10.1088/1742-6596/272/1/012001.

Choi, M. C., Raviv, U., Miller, H. P., Gaylord, M. R., Kiris, E., Ventimiglia, D., et al. (2009). Human microtubule-associated-protein tau regulates the number of protofilaments in microtubules: A synchrotron X-ray scattering study. *Biophysical Journal*, *97*(2), 519–527. http://dx.doi.org/10.1016/j.bpj.2009.04.047.

Chung, P. J., Choi, M. C., Miller, H. P., Feinstein, H. E., Raviv, U., Li, Y., et al. (2015). Direct force measurements reveal protein tau confers short-range attractions and isoform-dependent steric stabilization to microtubules. *Proceedings of the National Academy of Sciences of the United States of America*, *112*(47), E6416–E6425. http://dx.doi.org/10.1073/pnas.1513172112.

Chung, P. J., Song, C., Deek, J., Miller, H. P., Li, Y., Choi, M. C., et al. (2016). Tau mediates microtubule bundle architectures mimicking fascicles of microtubules found in the

axon initial segment. *Nature Communications*, *7*, 12278. Retrieved from, 10.1038/ncomms12278.

Cohen, J. A., & Highsmith, S. (1997). An improved fit to website osmotic pressure data. *Biophysical Journal*, *73*(3), 1689–1694. http://dx.doi.org/10.1016/S0006-3495(97)78200-6.

Cullity, B. D. (1957). Elements of x-ray diffraction. *American Journal of Physics*, *25*(6), 394. http://dx.doi.org/10.1119/1.1934486.

Deek, J., Chung, P. J., Kayser, J., Bausch, A. R., & Safinya, C. R. (2013). Neurofilament side-arms modulate parallel and crossed-filament orientations inducing nematic to isotropic and re-entrant birefringent hydrogels. *Nature Communications*, *4*, 2224. http://dx.doi.org/10.1038/ncomms3224.

Devanand, K., & Selser, J. C. (1991). Asymptotic behavior and long-range interactions in aqueous solutions of poly(ethylene oxide). *Macromolecules*, *24*(22), 5943–5947. http://dx.doi.org/10.1021/ma00022a008.

Dolan, P. J., & Johnson, G. V. W. (2010). The role of tau kinases in Alzheimer's disease. *Current Opinion in Drug Discovery & Development*, *13*(5), 595–603.

Drechsel, D. N., Hyman, A. A., Cobb, M. H., & Kirschner, M. W. (1992). Modulation of the dynamic instability of tubulin assembly by the microtubule-associated protein tau. *Molecular Biology of the Cell*, *3*(10), 1141–1154. http://dx.doi.org/10.1091/mbc.3.10.1141.

Ginsburg, A., Ben-Nun, T., Asor, R., Shemesh, A., Ringel, I., & Raviv, U. (2016). Reciprocal grids: A hierarchical algorithm for computing solution x-ray scattering curves from supramolecular complexes at high resolution. *Journal of Chemical Information and Modeling*, *56*(8), 1518–1527. http://dx.doi.org/10.1021/acs.jcim.6b00159.

Glatter, O., & Kratky, O. (Eds.), (1982). *Small-angle x-ray scattering*. London, UK: Academic Press.

Goode, B. L., Denis, P. E., Panda, D., Radeke, M. J., Miller, H. P., Wilson, L., et al. (1997). Functional interactions between the proline-rich and repeat regions of tau enhance microtubule binding and assembly. *Molecular Biology of the Cell*, *8*(2), 353–365. http://dx.doi.org/10.1091/mbc.8.2.353.

Himmler, A., Drechsel, D., Kirschner, M. W., & Martin, D. W. (1989). Tau consists of a set of proteins with repeated C-terminal microtubule-binding domains and variable N-terminal domains. *Molecular and Cellular Biology*, *9*(4), 1381–1388. http://dx.doi.org/10.1128/MCB.9.4.1381.Updated.

Kuznetsov, S. A., & Gelfand, V. I. (1986). Bovine brain kinesin is a microtubule-activated ATPase. *Proceedings of the National Academy of Sciences of the United States of America*, *83*(22), 8530–8534. http://dx.doi.org/10.1073/pnas.83.22.8530.

Lee, G., Cowan, N., & Kirschner, M. (1988). The primary structure and heterogeneity of tau protein from mouse brain. *Science*, *239*(4837), 285–288. http://dx.doi.org/10.1126/science.3122323.

Miller, H. P., & Wilson, L. (2010). Preparation of microtubule protein and purified tubulin from bovine brain by cycles of assembly and disassembly and phosphocellulose chromatography. *Methods in Cell Biology*, *95*(C), 2–15. http://dx.doi.org/10.1016/S0091-679X(10)95001-2.

Mitchison, T., & Kirschner, M. (1984). Dynamic instability of microtubule growth. *Nature*, *312*(5991), 237–242. http://dx.doi.org/10.1038/312237a0.

Needleman, D. J., Ojeda-Lopez, M. A., Raviv, U., Ewert, K., Jones, J. B., Miller, H. P., et al. (2004). Synchrotron x-ray diffraction study of microtubules buckling and bundling under

osmotic stress: A probe of interprotofilament interactions. *Physical Review Letters*, *93*(19), 198104. http://dx.doi.org/10.1103/PhysRevLett.93.198104.

Needleman, D. J., Ojeda-Lopez, M. A., Raviv, U., Ewert, K., Miller, H. P., Wilson, L., et al. (2005). Radial compression of microtubules and the mechanism of action of taxol and associated proteins. *Biophysical Journal*, *89*(5), 3410–3423. http://dx.doi.org/10.1529/biophysj.104.057679.

Needleman, D. J., Ojeda-Lopez, M. A., Raviv, U., Miller, H. P., Li, Y., Song, C., et al. (2013). Ion specific effects in bundling and depolymerization of taxol-stabilized microtubules. *Faraday Discussions*, *166*, 31–45. http://dx.doi.org/10.1039/c3fd00063j.

Needleman, D. J., Ojeda-Lopez, M. A., Raviv, U., Miller, H. P., Wilson, L., & Safinya, C. R. (2004). Higher-order assembly of microtubules by counterions: From hexagonal bundles to living necklaces. *Proceedings of the National Academy of Sciences of the United States of America*, *101*(46), 16099–16103. http://dx.doi.org/10.1073/pnas.0406076101.

Ojeda-Lopez, M. A., Needleman, D. J., Song, C., Ginsburg, A., Kohl, P. A., Li, Y., et al. (2014). Transformation of taxol-stabilized microtubules into inverted tubulin tubules triggered by a tubulin conformation switch. *Nature Materials*, *13*(2), 195–203. http://dx.doi.org/10.1038/nmat3858.

Parsegian, V. a., Fuller, N., & Rand, R. P. (1979). Measured work of deformation and repulsion of lecithin bilayers. *Proceedings of the National Academy of Sciences of the United States of America*, *76*(6), 2750–2754. http://dx.doi.org/10.1073/pnas.76.6.2750.

Parsegian, V. A., Rand, R. P., Fuller, N. L., & Rau, D. C. (1986). Osmotic stress for the direct measurement of intermolecular forces. *Methods in Enzymology*, *127*, 400–416. http://dx.doi.org/10.1016/0076-6879(86)27032-9.

Rand, R. P. (n.d.). Osmotic stress. Retrieved from www.brocku.ca/researchers/peter_rand/osmotic/osfile.html#data.

Raviv, U., Needleman, D. J., Li, Y., Miller, H. P., Wilson, L., & Safinya, C. R. (2005). Cationic liposome-microtubule complexes: Pathways to the formation of two-state lipid-protein nanotubes with open or closed ends. *Proceedings of the National Academy of Sciences of the United States of America*, *102*, 11167–11172. http://dx.doi.org/10.1073/pnas.0502183102.

Raviv, U., Nguyen, T., Ghafouri, R., Needleman, D. J., Li, Y., Miller, H. P., et al. (2007). Microtubule protofilament number is modulated in a stepwise fashion by the charge density of an enveloping layer. *Biophysical Journal*, *92*(1), 278–287. http://dx.doi.org/10.1529/biophysj.106.087478.

Safinya, C. R., Chung, P. J., Song, C., Li, Y., Ewert, K. K., & Choi, M. C. (2016). The effect of multivalent cations and Tau on paclitaxel-stabilized microtubule assembly, disassembly, and structure. *Advances in Colloid and Interface Science*, *232*, 9–16.

Safinya, C. R., Deek, J., Beck, R., Jones, J. B., & Li, Y. (2015). Assembly of biological nanostructures: Isotropic and liquid crystalline phases of neurofilament hydrogels. *Annual Review of Condensed Matter Physics*, *6*, 113–136. http://dx.doi.org/10.1146/annurev-conmatphys-031214-014623.

Safinya, C. R., Raviv, U., Needleman, D. J., Zidovska, A., Choi, M. C., Ojeda-Lopez, M. A., et al. (2011). Nanoscale assembly in biological systems: From neuronal cytoskeletal proteins to curvature stabilizing lipids. *Advanced Materials*, *23*(20), 2260–2270. http://dx.doi.org/10.1002/adma.201004647.

Schweers, O., Schönbrunn-Hanebeck, E., Marx, A., & Mandelkow, E. (1994). Structural studies of tau protein and Alzheimer paired helical filaments show no evidence for

beta-structure. *The Journal of Biological Chemistry*, *269*(39), 24290–24297. Retrieved from http://www.ncbi.nlm.nih.gov/pubmed/7929085.

Stanley, C. B., & Strey, H. H. (2003). Measuring osmotic pressure of poly(ethylene glycol) solutions by sedimentation equilibrium ultracentrifugation. *Macromolecules*, *36*(18), 6888–6893. http://dx.doi.org/10.1021/ma034079e.

Trinczek, B., Biernat, J., Baumann, K., Mandelkow, E. M., & Mandelkow, E. (1995). Domains of tau protein, differential phosphorylation, and dynamic instability of microtubules. *Molecular Biology of the Cell*, *6*(12), 1887–1902.

Warren, B. E. (1990). X-ray diffraction. In *Analysis: Vol. 1*. New York, NY: Dover Publications, Inc. http://dx.doi.org/10.1007/s00134-010-1760-5.